

On the length distribution in bundles of polymerizing and depolymerizing actin filaments

Heinrich Freistühler¹, Christian Schmeiser², and Nikolaos Sfakianakis³

¹University of Konstanz, Germany

²University of Vienna, Austria

³RICAM Vienna, Austria

September 15, 2010

Abstract

A model for the dynamics of the length distribution in polymer bundles is presented. It considers nucleation, polymerization, and depolymerization and is derived as a continuous macroscopic limit from a discrete description. Its main feature is a nonlinear coupling due to competition of the depolymerizing ends for the limited supply of a depolymerization agent. The model takes the form of an initial-boundary value problem for a one-dimensional nonlinear hyperbolic conservation law, subject to a nonlinear, nonlocal boundary condition. Besides existence and uniqueness of entropy solutions, convergence to a steady state is proven. Technical difficulties are caused by the fact that the prescribed boundary data are not always assumed by entropy solutions.

1 Introduction

The motility of a number of species of living cells is driven by polymerization and depolymerization of the protein *actin* in the *lamellipodium*, a thin sheet-like protrusive structure [SSVR02]. During phases of steady motion, which can be rather long for certain types of cells (e.g. the fish keratocyte), the shape of the lamellipodium does not change much, indicating a stable, stationary length distribution of actin filaments (polymerized actin). In recent mathematical models of lamellipodium dynamics [ÖS09], knowledge of the length distribution is required as input datum.

Actin filaments are polar. Almost all so called *barbed ends* are oriented towards the leading edge of the lamellipodium, and polymerization dominates there. A stationary length distribution therefore requires depolymerization at the opposite *pointed ends*. Both polymerization and depolymerization are regulated by proteins. Typical examples are *cofilin*, which drives filament severing (i.e. cutting off filament pieces), and *gelsolin*, which drives depolymerization by removing monomers one-by-one from pointed ends. It has been suggested [RBM⁺08] that the combination of polymerization at the barbed ends and of stochastic severing can lead to a stationary length distribution. This claim has been proven for a mathematical model [Fla08].

It is less clear that the action of gelsolin, i.e. one-by-one removal of monomers, can produce stationary length distributions. It seems that this would require a synchronization of polymerization at the barbed ends and depolymerization at the pointed ends, which is not very plausible. It has been suggested in [Fla08] that this synchronization can be replaced by an interaction between pointed ends in the form of a competition for a limited supply of gelsolin.

One of the objectives of this work and the subject of the following section is to derive a mathematical model under the following assumptions: A) Ensembles of parallel filaments are considered,

whose barbed ends are aligned. They are closely packed such that the pointed ends of equally long filaments are close together. B) At the barbed ends, polymerization occurs with the same rate for all filaments. C) At the pointed ends, depolymerization is triggered by gelsolin. It occurs in two steps: 1) one free molecule of gelsolin binds to a free pointed end; 2) one actin monomer is removed from the filament, and the gelsolin molecule and the pointed end become free again. The main modeling assumption is that this process is limited by the availability of gelsolin. The sum of the densities of free and bound gelsolin molecules is a prescribed constant. Pointed ends of filaments with the same length are in competition for gelsolin.

Since depolymerization at the pointed ends might be faster than polymerization at the barbed ends, filaments might be completely depolymerized, reducing the total number of filaments. We assume, however, that at the position of the barbed ends a fixed number of nucleation agents (NAs) is available, such that, whenever the filament number becomes smaller, free NAs nucleate new filaments. A candidate for the role of NA is the Arp2/3 complex occurring at the leading edge of lamellipodia [SXPM99].

In the following section, a discrete model is presented, where the distribution of polymer filaments with respect to the number of monomers is accounted for. A macroscopic continuous limit leads to a nonlinear hyperbolic conservation law for the density of pointed ends, as a function of distance from the barbed ends. The non-standard feature of the problem is a nonlocal boundary condition describing nucleation of new polymers. In Section 3, the theory of LeFloch [LeF88] is employed to deduce existence and uniqueness of an entropy solution of the initial-boundary value problem. The main result is large time convergence to a steady state, which is independent from the initial data and which corresponds to a linearly decreasing length distribution with compact support. A slight generalization of the model, where the total number of filaments can be above a preferred equilibrium, leads to a situation, where the boundary condition has to be interpreted in the generalized sense of Bardos [BLN79]. Existence and uniqueness of a solution is proven in Section 4 by a fixed point iteration. It is also shown that, after finite time, the boundary condition is assumed in the classical sense, which again allows to deduce convergence to the steady state. In Section 5, results of numerical experiments are presented, showing rather complex transient behaviour depending on the initial data.

2 Derivation of the model

The one-dimensional variable $x \geq 0$ stands synonymously for filament length as well as for the position along the filament bundle, where $x = 0$ denotes the common position of the barbed ends. Denoting the number of monomers per filament length by $1/l_m$, l_m can be interpreted as the 'length' of a monomer. Possible filament lengths (or pointed end positions) are then given by $x_j = j l_m$, $j \geq 1$. The number of filaments of length x_j at time t is denoted by $l_m u_j(t)$.

The number of filaments with length at least x_j is given by

$$\eta_j(t) = \sum_{i \geq j} l_m u_i(t)$$

and has the form of a Riemann sum with integrand u_i ; hence u_i can be interpreted as the number of filament ends per unit length. Accordingly, the total number of filaments is given by

$$N(t) = \eta_1(t).$$

The pointed end density $u_j = u_{f,j} + u_{b,j}$ is split into the density $u_{f,j}(t)$ of free pointed ends and the density $u_{b,j}(t)$ of pointed ends bound to a gelsolin molecule. We also introduce the density $\rho_{f,j}(t)$ of free gelsolin molecules at position x_j and time t , and note that $u_{b,j}(t)$ can also be interpreted as the density of bound gelsolin molecules. According to the assumption C) of the introduction, we require

$$\rho_{f,j}(t) + u_{b,j}(t) = \bar{\rho} \tag{1}$$

with a fixed (positive) constant $\bar{\rho}$. The dynamics of the pointed end densities is governed by the system

$$\frac{du_{b,j}}{dt} = k_b u_{f,j} \rho_{f,j} - k_d u_{b,j} + k_p (u_{b,j-1} - u_{b,j}), \quad (2)$$

$$\frac{du_{f,j}}{dt} = -k_b u_{f,j} \rho_{f,j} + k_d u_{b,j+1} + k_p (u_{f,j-1} - u_{f,j}), \quad (3)$$

The first terms on the right hand sides describe the binding of free gelsolin molecules and free pointed ends with rate k_b . The second terms describe the reverse reaction, which also involves depolymerization by one monomer with rate k_d . The third terms model the elongation of filaments by polymerization by one monomer at the plus-ends with rate k_p .

We introduce a nondimensionalization of (1)–(3), where $\bar{\rho}$ is used as reference value for the densities $\rho_{f,j}$, $u_{b,j}$, and $u_{f,j}$. A macroscopic length scale l , much bigger than the monomer length l_m , is used as reference length. The reference time is $l/(l_m k_d)$. Using the same symbols for the dimensionless variables, we arrive at the scaled system

$$\rho_{f,j} + u_{b,j} = 1, \quad (4)$$

$$\varepsilon \frac{du_{b,j}}{dt} = \alpha u_{f,j} \rho_{f,j} - u_{b,j} + \varepsilon v_p \frac{u_{b,j-1} - u_{b,j}}{\varepsilon}, \quad (5)$$

$$\varepsilon \frac{du_{f,j}}{dt} = -\alpha u_{f,j} \rho_{f,j} + u_{b,j} + \varepsilon \frac{u_{b,j+1} - u_{b,j}}{\varepsilon} + \varepsilon v_p \frac{u_{f,j-1} - u_{f,j}}{\varepsilon}, \quad (6)$$

with the dimensionless parameters

$$\alpha = \frac{k_b \bar{\rho}}{k_d}, \quad v_p = \frac{k_p}{k_d}, \quad \varepsilon = \frac{l_m}{l} \ll 1. \quad (7)$$

Note that, for the scaled pointed end positions, $x_{j+1} - x_j = \varepsilon$ holds. The scaling assumption that the rates of the binding reaction, of the depolymerization reaction, and of the polymerization reaction are of the same order of magnitude, implies that the scaled binding reaction α and the scaled polymerization speed v_p take moderate values.

As a preparation for the continuous limit $\varepsilon \rightarrow 0$, we state the equation

$$\frac{du_j}{dt} + v_p \frac{u_j - u_{j-1}}{\varepsilon} - \frac{u_{b,j+1} - u_{b,j}}{\varepsilon} = 0, \quad (8)$$

for the total pointed end density

$$u_j = u_{b,j} + u_{f,j}. \quad (9)$$

Assuming that there are smooth functions $\rho_f(t, x)$ and $u(t, x) = u_b(t, x) + u_f(t, x)$ such that $\rho_{f,j}(t)$ approximates $\rho_f(t, x_j)$ for small ε and analogously for the other variables, the formal limit $\varepsilon \rightarrow 0$ of (4), (9), (5), (8) leads to the problem

$$\begin{aligned} \rho_f + u_b &= 1, & u_f + u_b &= u, & u_b &= \alpha u_f \rho_f, \\ \partial_t u + \partial_x (v_p u - u_b) &= 0. \end{aligned}$$

Computing u_b as a function of u from the first three equations, the problem can be reduced to a nonlinear hyperbolic conservation law:

$$\partial_t u + \partial_x f(u) = 0, \quad \text{with } f(u) = v_p u - \frac{1}{2} \left(u + \frac{1}{\alpha} + 1 - \sqrt{\left(u + \frac{1}{\alpha} + 1 \right)^2 - 4u} \right). \quad (10)$$

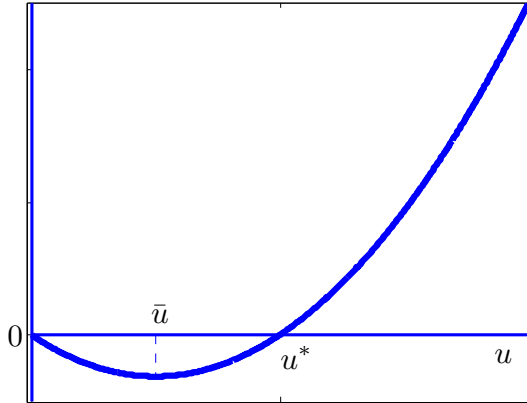


Figure 1: The graph of the flux function f . It is smooth, convex, with two roots $0, u^*$ and a minimum $\bar{u} \in (0, u^*)$.

The flux function f has the properties

$$f'' > 0, \quad f'(0) = v_p - \frac{\alpha}{\alpha + 1}, \quad f(u) = v_p u - 1 + O(u^{-1}) \text{ as } u \rightarrow \infty,$$

and a typical graph is presented in Figure 1.

The last property shows that polymerization dominates for large pointed end densities. On the other hand, we assume that depolymerization wins for small values of u :

$$v_p < \frac{\alpha}{\alpha + 1}. \quad (11)$$

In this case,

$$f(0) = f(\bar{u}) = f(u^*) = 0 \quad \text{for} \quad 0 < \bar{u} = 1 - \frac{1}{\alpha} + \frac{1 - 2v_p}{\sqrt{\alpha v_p(1 - v_p)}} < u^* = \frac{\alpha - v_p(1 + \alpha)}{\alpha v_p(1 - v_p)}. \quad (12)$$

Remark 1. Before proceeding, we note that due to (7), relation (11) yields a condition on the dimensional rates k_p, k_d, k_b that govern the competitive dynamics of polymerization and depolymerization. For this discussion we refer to the last paragraph of this work.

Nucleation – auxiliary conditions: The total number of filaments is given by

$$N(t) = \int_0^\infty u(t, x) dx.$$

The barbed ends are assumed to be tied to nucleation agents (NA), whose total number $\bar{N} > 0$ is fixed, implying $N(t) \leq \bar{N}$. We assume that free NA nucleate new filaments with a rate $1/\tau_n$, which can be translated as a flux of pointed ends at $x = 0$. In the nondimensionalization above, the choice of the length scale l has not been fixed so far. We make up for this by requiring the characteristic time $l/(l_m k_d)$ to be equal to τ_n , i.e. $l = l_m k_d \tau_n$. The small parameter can now be written as $\varepsilon = 1/(k_d \tau_n)$ with the interpretation that the nucleation process is much slower than the depolymerization reaction. In the nondimensionalized setting, our considerations result in the nonlocal boundary condition

$$f(u(t, 0)) = \bar{N} - \int_0^\infty u(t, x) dx.$$

Since the right hand side is nonnegative and $f : [u^*, \infty) \rightarrow [0, \infty)$ is strictly increasing and possesses the inverse φ , the boundary condition can be written as

$$u(t, 0) = \varphi \left(\bar{N} - \int_0^\infty u(t, x) dx \right) \geq u^*, \quad t > 0. \quad (13)$$

The problem (10), (13) is completed by prescribing initial data:

$$u(0, x) = u_0(x) \geq 0, \quad x > 0. \quad (14)$$

Assuming that u_0 has compact support, the same is true for $u(t, \cdot)$ for $t > 0$ by the finite propagation speed. By integration of the conservation law (10) with respect to x (for a solution with compact support) and by using the boundary condition, the simple ODE

$$\frac{dN}{dt} = \bar{N} - N \quad (15)$$

is derived. Together with the initial condition (14) this implies

$$N(t) = \bar{N} + \left(\int_0^\infty u_0(x) dx - \bar{N} \right) e^{-t}. \quad (16)$$

3 Existence, uniqueness, and convergence to a steady state

If the formal computations at the end of the previous section are justified, then the problem reduces to a standard initial-boundary value problem with prescribed boundary data

$$u(t, 0) = u_b(t) := \varphi(\bar{N} - N(t)), \quad (17)$$

with $N(t)$ given by (16) and, consequentially, $u_b(t) \rightarrow u^*$ exponentially fast as $t \rightarrow \infty$.

The justification of (17) is nontrivial, however, since solutions of hyperbolic conservation laws cannot be expected to assume given boundary values in general. The generally accepted solution concept, which can be justified by a vanishing viscosity approach, is due to [BLN79]. It states that the boundary condition should be replaced by

$$\begin{aligned} u(t, 0+) &= b_m(t) := \max\{\bar{u}, u_b(t)\}, \\ \text{or} \quad f'(u(t, 0+)) &\leq 0 \quad \text{and} \quad f(u(t, 0+)) \geq f(b_m(t)), \end{aligned}$$

where $u(t, 0+)$ denotes the trace of u at $x = 0$. We note that the max that appears in the first line does not constitute a restriction, and that the second line describes the situation, where the boundary condition $b_m(t)$ is not assumed by the solution.

With the properties of the flux function f and of the boundary datum u_b given in the previous section, the above conditions always reduce to (17). This is easily seen, since $u_b > u^*$ so $b_m = u_b$; hence $f(b_m) \geq 0$ (cf Figure 1) and the second line of the boundary condition is not valid.

By the boundedness and continuity of u_b , the results of [LeF88] imply existence and uniqueness of a global entropy solution of (10), (14), (16), (17) and, thus, of (10), (13), (14).

As a preparation for the long time asymptotics, we show that u can be obtained as the solution of a Cauchy problem. However, this process typically cannot be started at $t = 0$, but only at a large enough time T_1 . The backward characteristic

$$x = (t - \tau)f'(u_b(\tau))$$

through the point $(t, x) = (\tau, 0)$, $\tau > T_1$, carrying the value $u_b(\tau)$ intersects the line $t = T_1$ at

$$x = Y(\tau) := (T_1 - \tau)f'(u_b(\tau)) < 0.$$

The derivative $Y'(\tau) = -f'(u_b(\tau)) + (T_1 - \tau)f''(u_b(\tau))u'_b(\tau)$ can be estimated by

$$Y'(\tau) \leq -f'(u_b(\tau)) + c\tau|u'_b(\tau)| \xrightarrow{\tau \rightarrow \infty} -f'(u^*) < 0,$$

because of the exponential decay of u'_b . The constant c is a bound for f'' on $[\bar{u}, u^*]$. This implies that Y is strictly monotonically decreasing on $[T_1, \infty)$ for large enough T_1 .

The appropriate definition for the Cauchy data therefore is

$$u_C(x) := \begin{cases} u_b(Y^{-1}(x)) & \text{for } x < 0 \\ u(T_1, x) & \text{for } x > 0. \end{cases}$$

In other words, the solution of the initial-boundary value problem for $t \geq T_1$ can be computed by solving the Cauchy problem

$$\partial_t u + \partial_x f(u) = 0, \quad \text{for } t > T_1, \quad u(T_1, x) = u_C(x), \quad (18)$$

and by restricting the solution to $x > 0$.

Since $u_b(t) - u^* = O(e^{-t})$ as $t \rightarrow \infty$,

$$Y(t) \approx -tf'(u^*) \quad \text{as } t \rightarrow \infty.$$

As a consequence,

$$u_C(x) - u^* = O\left(\exp\left(\frac{x}{f'(u^*)}\right)\right) \quad \text{as } x \rightarrow -\infty. \quad (19)$$

The study of long time asymptotics for nonlinear hyperbolic conservation laws has a long history (see, e.g., [Liu77]). A typical result for Cauchy problems is the following.

Lemma 1. *Let $f'' > 0$, $f(0) = f(u^*) = 0$ with $0 < u^*$, let*

$$u_\infty(x) = \begin{cases} u^* & \text{for } x < x_\infty, \\ 0 & \text{for } x > x_\infty, \end{cases} \quad (20)$$

let $u_I - u_\infty \in L^1(\mathbb{R}) \cap L^\infty(\mathbb{R})$, and let

$$\int_{\mathbb{R}} (u_I - u_\infty) dx = 0.$$

Then the solution u of (18) for $u_C = u_I$ satisfies

$$\lim_{t \rightarrow \infty} \|u(t, \cdot) - u_\infty\|_{L^1(\mathbb{R})} = 0.$$

Since the restriction of u to $x > 0$ solves the initial-boundary value problem (10)–(14), x_∞ can be determined from the requirement

$$\bar{N} = N(\infty) = \int_0^\infty u_\infty dx = u^* x_\infty.$$

We collect the results of this section:

Theorem 2. *Let (11) hold, let $0 \leq u_0 \in L^1(\mathbb{R}^+) \cap L^\infty(\mathbb{R}^+)$ have compact support and satisfy*

$$\int_0^\infty u_0 dx \leq \bar{N}. \quad (21)$$

Let φ be the inverse of $f : [u^, \infty) \rightarrow [0, \infty)$. Then the problem (10)–(14) has a global unique entropy solution u satisfying*

$$\lim_{t \rightarrow \infty} \|u(t, \cdot) - u_\infty\|_{L^1(\mathbb{R}^+)} = 0,$$

with u_∞ defined in (20) with $x_\infty = \bar{N}/u^$.*

4 A generalized model

In this section, we consider the more general case, in which $N(t)$ might be bigger than a preferred number of filaments. Such cases of oversaturation allow for situations in which, differently from above, the prescribed boundary conditions are not assumed at all times. This complicates the analysis significantly.

Consider the problem

$$\partial_t u + \partial_x f(u) = 0, \quad x, t > 0, \quad (22)$$

subject to the boundary condition

$$u(t, 0+) = u_b(t) := \psi \left(\int_0^\infty u(t, x) dx \right), \quad (23)$$

$$\text{or } f'(u(t, 0+)) \leq 0 \quad \text{and} \quad f(u(t, 0+)) \geq f(u_b(t)), \quad t > 0, \quad (24)$$

and to the initial condition

$$u(0, x) = u_0(x), \quad x > 0, \quad (25)$$

where the data satisfy

$$f \text{ smooth, } f'' > 0, \quad f(0) = f'(\bar{u}) = f(u^*) = 0, \quad f'(0) < 0 \quad \text{with } 0 < \bar{u} < u^*, \quad (26)$$

$$\psi : [0, \infty) \rightarrow [\bar{u}, \infty) \quad \text{Lipschitz, non-increasing,}$$

$$C^1 \text{ in a neighborhood of } \bar{N} > 0, \quad \psi(\bar{N}) = u^*, \quad \psi'(\bar{N}) < 0, \quad (27)$$

$$0 \leq u_0 \in L^\infty(\mathbb{R}^+) \quad \text{with compact support.} \quad (28)$$

Existence and uniqueness

The essential difference to the previous section, where \bar{N} was the maximum number of filaments the cell can sustain, in this section \bar{N} represents the preferable number of filaments, i.e. we do not assume (21) any more. This in turn allows for $u_b(t) < u^*$ and, thus, makes the alternative (24) of the boundary condition possible. Note that, if (23) holds, the total number of filaments solves the ODE

$$\frac{dN}{dt} = f(\psi(N)), \quad N(t) = \int_0^\infty u(t, x) dx, \quad (29)$$

which – similarly to (15) – has the unique, globally attractive steady state $N = \bar{N}$. However, since (23) cannot be guaranteed, $N(t)$ cannot be computed a priori by solving (29), so the existence and uniqueness of a solution is not a simple consequence of [LeF88] any more.

Theorem 3 (Global existence and uniqueness). *Let (26)–(28) hold. Then the problem (22)–(25) has a unique entropy solution $u \in C([0, \infty); L^1(\mathbb{R}^+))$, such that $u(t, \cdot)$ has compact support for every $t \geq 0$, and*

$$0 \leq u(t, x) \leq \max \left\{ \psi(0), \sup_{\mathbb{R}^+} u_0 \right\}, \quad \forall t, x > 0.$$

Proof. It suffices to prove local existence and uniqueness of a solution with the properties stated in the theorem, which imply that, for $t > 0$, the solution satisfies the assumptions (28) on the initial data and therefore can be continued.

For a given $T > 0$ we consider the Banach space

$$\mathcal{X}_T = C([0, T], L^1(\mathbb{R}^+)), \quad \text{equipped with} \quad \|u\|_{\mathcal{X}_T} = \max_{t \in [0, T]} \|u(t, \cdot)\|_{L^1(\mathbb{R}^+)},$$

and its closed subset

$$\mathcal{S}_T = \{u \in \mathcal{X}_T \mid 0 \leq u \leq u_{max}\}, \quad u_{max} := \max \left\{ \psi(0), \sup_{\mathbb{R}^+} u_0 \right\}.$$

We define a fixed point operator $\mathcal{P} : \mathcal{S}_T \rightarrow \mathcal{S}_T$ by $\mathcal{P}(v) = u$, where u solves (22)–(25) with the definition of the boundary data in (23) replaced by

$$u_b[v](t) := \psi \left(\int_0^\infty v(t, x) dx \right).$$

By (27) and $v \in \mathcal{X}_T$, $u_b[v]$ is continuous and bounded. This, together with (26)–(28) suffices for the application of Theorems 2.1 and 2.2 of [LeF88], guaranteeing that $\mathcal{P}(v) \in \mathcal{X}_T$ is well defined and that \mathcal{P} maps \mathcal{S}_T into itself.

Theorem 2.2 of [LeF88] also provides the stability estimate

$$\|\mathcal{P}(v_1)(t, \cdot) - \mathcal{P}(v_2)(t, \cdot)\|_{L^1(\mathbb{R}^+)} \leq \int_0^t |f(u_b[v_1](s)) - f(u_b[v_2](s))| ds \leq TL_f L_\psi \|v_1 - v_2\|_{\mathcal{X}_T},$$

where L_f is the Lipschitz constant of f on $[\bar{u}, \psi(0)]$ and L_ψ is the Lipschitz constant of ψ . This proves that \mathcal{P} is a contraction for small enough T and, thus, completes the existence and uniqueness proof.

Finally, by the finite speed of propagation, if $\text{supp}(u_0) \subset [0, \bar{x}]$ then

$$\text{supp}(u(t, \cdot)) \subset [0, \bar{x} + f'(u_{max})t].$$

□

Convergence to the steady state

For proving decay to equilibrium, it will suffice to show that the boundary data are assumed for large enough times, i.e. that there exists $T > 0$ such that (23) holds for $t > T$. Then the strategy of the previous section can be applied.

We shall need more details concerning the solution of the initial-boundary value problem. The basic idea of [LeF88] is to use the explicit representation of the entropy solution due to Lax [Lax57] for an equivalent Cauchy problem as derived in the previous section. Complications arise, however, due to the different alternatives in the boundary conditions.

We shall need the Legendre transform

$$g(v) = \sup_{u \in \mathbb{R}} (uv - f(u)) = vb(v) - f(b(v)), \quad b := (f')^{-1},$$

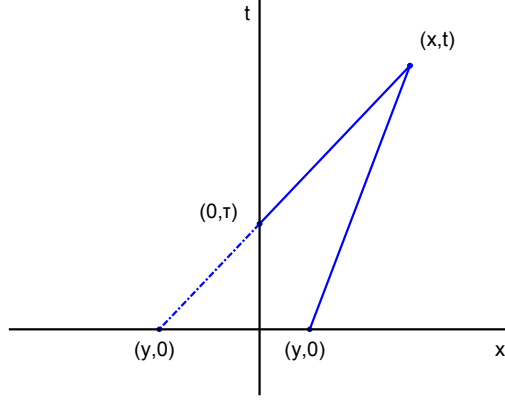


Figure 2: For a given (x, t) the minimizer y of $G(y, t, x)$ can be $y \geq 0$ or $y \leq 0$. In both cases the slope of the line connecting (x, t) with $(y, 0)$ is given by the solution formula: $u(t, x) = (f')^{-1}\left(\frac{x-y}{t}\right)$, $y \in \mathbb{R}$, and reads $\frac{t}{x-y} = \frac{1}{f'(u(t, x))}$. In the case $y \leq 0$, τ represents the intersection point of the straight line $(x, t) - (y, 0)$ with the boundary $x = 0$; that is $\frac{x-y}{t} = \frac{x}{t-\tau}$.

of the flux function. As a consequence of (26), g has the properties

$$g \text{ smooth}, \quad g'' > 0, \quad g(c) = g'(c) = 0, \text{ for } c := f'(0) < 0, \quad g'(v) = b(v). \quad (30)$$

The solution of (22)–(25) can then be written as ([LeF88], see also [JG91])

$$u(t, x) = b\left(\frac{x - y(t, x)}{t}\right), \quad \text{with } y(t, x) = \operatorname{argmin}_{y \in \mathbb{R}} G(y; t, x),$$

where

$$G(y; t, x) = \begin{cases} \int_0^y u_0(\xi) d\xi + t g\left(\frac{x-y}{t}\right), & y \geq 0, \\ -\int_0^{yt/(y-x)} \mathcal{Y}(s) ds + \frac{xt}{x-y} g\left(\frac{x-y}{t}\right), & y \leq 0. \end{cases}$$

The definition of the function \mathcal{Y} involves the solution of a variational inequality. Its details will not be needed in the following. It is interesting to note, however, that $\mathcal{Y}(t) = f(u(t, 0+))$ holds for the solution.

It is easily seen that, for continuous u_0 and $y(t, x) > 0$, $u(t, x) = u_0(y(t, x))$ holds. Similarly, if the boundary data are assumed (i.e. (23) holds) and continuous then, for $y(t, x) < 0$, $u(t, x) = u_b(\tau(t, x))$ holds with

$$\frac{x - y(t, x)}{t} = \frac{x}{t - \tau(t, x)}.$$

For a fixed (t, x) we produce a curve $C_{t,x} = \{(\tau, y_\tau(t, x)) : 0 \leq \tau \leq t\}$ connecting $y_0(t, x) = y(t, x)$ and $y_t(t, x) = x$ by replacing t by $t - \tau$ and u_0 by $u(\tau, \cdot)$ in the definition of G and computing the minimizers, and we refer to Figure 2 for a graphical explanation.

We call $C_{t,x}$ the *backward characteristic* through (t, x) emanating from $y(t, x)$. For smooth solutions backward characteristics are classical characteristics with equation $x = y + tf'(u_0(y))$ if $y > 0$, or $x = (t - \tau)f'(u_b(\tau))$ if $y < 0$.

We start by proving that for large enough t and for arbitrary $x > 0$, $C_{t,x}$ cannot emanate from the support of u_0 .

Lemma 4. *Let (26)–(28) hold and $\text{supp}(u_0) \subset [0, \bar{x}]$. Then there exists $T_2 > 0$, such that $y(t, x) \notin (0, \bar{x})$ for all $x > 0$, $t > T_2$.*

Proof. Let $t, x > 0$ be such that $0 \leq \eta := y(t, x) < \bar{x}$. Then, in view of (30),

$$\frac{x - \eta}{t} > -\frac{\bar{x}}{t} > c,$$

for t large enough. Since, again by (30), g is increasing on $[c, \infty)$ and $g(0) = -f(\bar{u}) > 0$, there exists $\bar{t} > 0$ (independent of x) such that

$$g\left(\frac{x - \eta}{t}\right) \geq g\left(-\frac{\bar{x}}{t}\right) \geq -\frac{f(\bar{u})}{2} \quad \text{for every } t \geq \bar{t}.$$

This in turn implies that for every $t \geq \bar{t}$

$$G(\eta; t, x) \geq -\frac{f(\bar{u})}{2} t, \quad (31)$$

since $\eta = y(t, x) \geq 0$. Moreover, since $x - tc > 0$ and since η is the minimizer of $G(\cdot; t, x)$,

$$G(\eta; t, x) \leq G(x - tc; t, x) = \int_0^{x-tc} u_0(\xi) d\xi + tg(c) \leq K, \quad (32)$$

where the last inequality stems from (28), using $g(c) = 0$ and $K = \text{diam}(\text{supp}(u_0)) \|u_0\|_{L^\infty}$.

Combination of (31) and (32) implies that we arrive at a contradiction for $t > T_2 := \max\{\bar{t}, -2K/f(\bar{u})\}$, which completes the proof. \square

Lemma 5. *Let the assumptions of Lemma 4 hold. Then (23) holds for $t > T_2$ with $T_2 > 0$ from Lemma 4.*

Proof. We distinguish between two cases:

Case 1: Assume for a $t \geq 0$, $N(t) < \bar{N}$. Then, by the continuity of $N(t)$, this remains true at least for a small time interval. Since, in this interval, $u_b(t) > u^*$, (23) and, consequently, the ODE (29) hold there. This in turn implies that $N(t) < \bar{N}$ and, thus, (23) remains true for all times. This is actually the setting of the previous section.

Case 2: Assume that for a $t > T_2$, $N(t) \geq \bar{N}$ holds. For $x \in (0, \bar{N}/u_{max})$ (where u_{max} is given in Theorem 3 and is an upper bound of the solution u) assume $y(t, x) > \bar{x}$. Then, since

$$G(y; t, x) = \int_0^\infty u_0(\xi) d\xi + tg\left(\frac{x - y}{t}\right)$$

in a neighbourhood of $y = y(t, x)$, the minimum satisfies $dG/dy = 0$; hence

$$u(t, x) = b\left(\frac{x - y(t, x)}{t}\right) = 0.$$

By the monotonicity of $y(t, x)$ with respect to x (Proposition 2.4 in [LeF88]), $u(t, x') = 0$ holds for $x' \geq x$. As a consequence $N(t) \leq xu_{max} < \bar{N}$ in contradiction to the basic assumption of this case. Therefore, $y(t, x) \leq 0$ follows from Lemma 4, implying $\frac{x - y(t, x)}{t} > 0$ and since $b \nearrow$ in $[0, \infty)$, it reads

$$u(t, x) = b\left(\frac{x - y(t, x)}{t}\right) > b(0) = \bar{u} \quad \text{for } x < \bar{N}/u_{max}.$$

The consequence $u(t, 0+) \geq \bar{u}$ excludes (24), completing the proof. \square

For proving convergence to the steady state it suffices to repeat the argument of the preceding section with a T_1 satisfying the additional requirement $T_1 \geq T_2$.

Theorem 6. *Let (26)–(28) hold. Then the entropy solution u of (22)–(25) satisfies*

$$\lim_{t \rightarrow \infty} \|u(t, \cdot) - u_\infty\|_{L^1(\mathbb{R}^+)} = 0,$$

with u_∞ defined in (20) with $x_\infty = \bar{N}/u^*$.

Remark 2. The steady state solution is independent from the initial conditions. With respect to the flux function, it depends only on its root, and with respect to the boundary condition it depends only on the ‘preferred’ number of filaments \bar{N} .

5 Numerical experiments

For the numerical tests we note that the finite speed of propagation and the convergence of the solution u to a steady state with bounded support guarantee that $\mathcal{S} = \bigcup_{t \geq 0} \text{supp}(u(t, \cdot)) \subset \mathbb{R}^+$ is finite. So, for the needs of the numerical tests we shall consider a finite computational domain $[0, x_{num}]$ satisfying $[0, x_{num}] \supset \mathcal{S}$.

We discretize the spatial computational domain $[0, x_{num}]$ by a fixed-in-time, uniform-in-space grid with N_x points:

$$\mathcal{D}_x = \left\{ x_i = (i-1)\Delta x \mid i = 1, \dots, N_x, \Delta x = \frac{x_{num}}{N_x - 1} \right\}.$$

The temporal domain is discretized as

$$\mathcal{D}_t = \left\{ t^n = t^{n-1} + \Delta t^n \mid n = 1, \dots, N_t, t^0 = 0 \right\},$$

where the time steps Δt^n are chosen such that the CFL condition is satisfied. The maximum time step N_t is chosen sufficiently large so that the problem under consideration reaches its steady state.

The numerical solution at the time step t^n is denoted by

$$U^n = \left\{ u_i^n \mid i = 1, \dots, N_x \right\},$$

where u_i^n are discrete approximations of the cell averages of the exact solution, i.e

$$u_i^n \approx \frac{1}{\Delta x} \int_{x_i}^{x_{i+1}} u(x, t^n) dx, \quad i = 1, \dots, N_x, \quad n = 1, \dots, N_t.$$

The numerical solution is computed as follows:

- For $i = 1$, the computation of the numerical solution, depends on the boundary conditions and is described in the paragraphs that follow.
- For $i = 2, \dots, N_x - 1$, the numerical solution is computed using an explicit in time conservative Finite Volume scheme

$$u_i^{n+1} = u_i^n - \frac{\Delta t^n}{\Delta x} \left(F_{i+1/2}^n - F_{i-1/2}^n \right).$$

For the computation of the numerical flux we use the superbee flux limiter:

$$\begin{aligned} F_{i+1/2}^n &= F_{i+1/2}^{n,LxF} - \rho(r_i^n) \left(F_{i+1/2}^{n,LxF} - F_{i+1/2}^{n,Rchtmr} \right) \\ F_{i-1/2}^n &= F_{i-1/2}^{n,LxF} - \rho(r_{i-1}^n) \left(F_{i-1/2}^{n,LxF} - F_{i-1/2}^{n,Rchtmr} \right) \end{aligned}$$

where the flux limiter function ρ is defined by

$$r_i^n = \frac{u_i^n - u_{i-1}^n}{u_{i+1}^n - u_i^n}$$

$$\rho(r) = \max\{0, \min\{2r, 1\}, \min\{r, 2\}\}$$

and the numerical fluxes used as building block are the Lax-Friedrichs flux and the Richtmyer flux

$$F_{i+1/2}^{n,LxF} = \frac{f(u_i^n) + f(u_{i+1}^n)}{2} - \frac{\Delta x}{2\Delta t^n}(u_{i+1}^n - u_i^n),$$

$$F_{i+1/2}^{n,Rchtmr} = f\left(\frac{u_i^n + u_{i+1}^n}{2} - \frac{\Delta t^n}{2\Delta x}(f(u_i^n) - f(u_{i+1}^n))\right).$$

For more details on flux limiters, we refer to [LeV04].

- For $i = N_x$, we use that the computational domain satisfies $[0, x_{num}] \supset \mathcal{S}$ and we set

$$u_{N_x}^{n+1} = u_{N_x}^n.$$

In the following numerical tests, the spatial mesh is discretized using $N_x = 2000$ grid points, and the time steps Δt^n are chosen such as the Courant number is 0.9

$$\frac{\Delta t^n}{\Delta x} \max_i |f'(u_i^n)| = 0.9.$$

Numerical test 1. This numerical test refers to the initial model as in Theorem 2. In this case the evolution of the total mass $N(t)$ is given by (16), and the boundary condition by (17). So at every time step t^{n+1} we compute

$$N^{n+1} = N(t^{n+1}),$$

and u_1^{n+1} by solving the nonlinear problem

$$f(u_1^{n+1}) = \bar{N} - N^{n+1}.$$

So the numerical scheme is

$$\text{Sch1} :: \begin{cases} f(u_1^{n+1}) = \bar{N} - N^{n+1}, & i = 1, \\ u_i^{n+1} = u_i^n - \frac{\Delta t}{\Delta x} (F_{i+1/2}^n - F_{i-1/2}^n), & i = 2, \dots, N_x - 1 \\ u_{N_x}^{n+1} = u_{N_x}^n, & i = N_x \end{cases} .$$

The parameters used in this case are

$$\text{Par1} :: \begin{cases} u_0(x) = 0, & x > 0, \\ f(u) = u(u - 2), & (u^* = 2) \\ \bar{N} = 30 \end{cases} .$$

We refer to Figure 3 for a graphical representation of this test case.

Numerical test 2. This numerical test refers to the generalized model case as summarized in Theorem 6.

In this case the boundary condition is given by (23) or (24). At every time step t^n we compute the boundary function u_b by using (23) and the trace u_{tr} by extrapolation of the values u_3^n, u_4^n to the boundary, i.e

$$u_b(t^n) = \psi \left(\Delta x \sum_{i=1}^{N_x} u_i^n \right),$$

$$u_{tr}(t^n) = 3u_3^n - 2u_4^n$$

respectively. We then use (24) for $u_b(t^n)$ and $u_{tr}(t^n)$ to decide whether the boundary function value is attained, and we set

$$u_1^{n+1} = \begin{cases} u_b(t^n), & \text{if } u_b(t^n) \text{ is assumed} \\ u_1^n - \frac{\Delta t^n}{\Delta x} (f(u_2^n) - f(u_1^n)), & \text{if } u_b(t^n) \text{ is not assumed} \end{cases}.$$

The numerical scheme is

$$\text{Sch2} :: \begin{cases} u_1^{n+1}, & i = 1, \\ u_i^{n+1} = u_i^n - \frac{\Delta t}{\Delta x} (F_{i+1/2}^n - F_{i-1/2}^n), & i = 2, \dots, N_x - 1 \\ u_{N_x}^{n+1} = u_{N_x}^n, & i = N_x \end{cases}.$$

The parameters used are

$$\text{Par2} :: \begin{cases} u_0(x) = 0, & x > 0, \\ f(u) = e^u - \frac{e^2 - 1}{2} u - 1, & (u^* = 2) \\ \psi = 2 \exp \left(\frac{\bar{N} - \int_0^\infty u(t,x) dx}{20} \right), \\ \bar{N} = 10 \end{cases}.$$

We refer to Figure 4 for a graphical representation of this test case.

Numerical test 3. In this numerical test, we examine the dependence of the steady state solutions on the polymerization/depolymerization rate ratio v_p .

We use (7), and assume that the binding/depolymerization ratio $\alpha = \frac{k_b \bar{p}}{k_d}$ is constant, while we allow for variable $v_p = \frac{k_p}{k_d}$. The numerical scheme that we use is the same as in the Numerical test 1 case, with flux function given by the modeling approach (10)

$$f(u) = v_p u - \frac{1}{2} \left(u + \frac{1}{\alpha} + 1 - \sqrt{\left(u + \frac{1}{\alpha} + 1 \right)^2 - 4u} \right).$$

The flux functions that we consider satisfy the conditions (12), more specifically their root u^* depends on α and v_p as

$$u^* = \frac{\alpha - v_p(1 + \alpha)}{\alpha v_p(1 - v_p)}.$$

The respective steady state profiles are given by (20) and Theorem 2, namely

$$u_\infty(x) = \begin{cases} u^* & \text{for } x < x_\infty, \\ 0 & \text{for } x > x_\infty, \end{cases},$$

with $x_\infty = \frac{\bar{N}}{u^*}$.

We also note, for the curve (x_∞, u^*) , that $\lim_{v_p \rightarrow \frac{\alpha}{\alpha+1}} u^* = 0$; hence $\lim_{v_p \rightarrow \frac{\alpha}{\alpha+1}} x_\infty = \infty$, and that $\lim_{v_p \rightarrow 0} u^* = \infty$; hence $\lim_{v_p \rightarrow 0} x_\infty = 0$.

For this test, we choose $\bar{N} = 100$, $\alpha = 1$ and we compute the steady state solutions for various values of v_p that satisfy the restriction (11)

$$v_p < \frac{\alpha}{\alpha + 1} = \frac{1}{2}.$$

The results of this test are presented in Figure (5).

Numerical test 4. In this numerical test we examine the dependence of the steady state solution on the binding/depolymerization rate ratio α , while keeping v_p fixed. The computational setting (numerical scheme, flux function) is as described in the paragraph **Numerical test 3**.

We note, due to (11), that

$$0 < v_p < 1, \quad \alpha > \frac{v_p}{1 - v_p},$$

and due to (12) that

$$u^* = \frac{1}{v_p} - \frac{1}{1 - v_p} \frac{1}{\alpha}$$

So

$$u^* \longrightarrow \begin{cases} \frac{1}{v_p}, & \text{as } \alpha \rightarrow +\infty \\ 0, & \text{as } \alpha \rightarrow \frac{v_p}{1 - v_p} \end{cases}$$

and the maximum length of filaments

$$x_\infty = \frac{\bar{N}}{u^*} \longrightarrow \begin{cases} \bar{N} v_p, & \text{as } \alpha \rightarrow +\infty \\ +\infty, & \text{as } \alpha \rightarrow \frac{v_p}{1 - v_p} \end{cases}$$

For this test, we choose $\bar{N} = 100$, $v_p = \frac{1}{4}$ and we compute the steady state solutions and respective length distributions, for various values of α that satisfy

$$\alpha > \frac{v_p}{1 - v_p} = \frac{1}{3}.$$

The results of this test are presented in Figure (6).

6 Conclusions

With the model derived in Section 2, the dimensional version of the stationary length distribution

$$\eta_\infty(x) = \int_x^\infty u_\infty(x) dx$$

is given by

$$\eta_\infty(x) = \bar{N} - x \frac{k_d[k_b \bar{\rho} k_d - k_p(k_d + k_b \bar{\rho})]}{k_b k_p(k_d - k_p)},$$

for

$$x \leq x_\infty = \frac{\bar{N} k_b k_p(k_d - k_p)}{k_d[k_b \bar{\rho} k_d - k_p(k_d + k_b \bar{\rho})]},$$

and $\eta_\infty(x) = 0$ for $x > x_\infty$. This result can be used as input when modeling cytoskeleton dynamics [ÖS09] under the assumption that the dynamic processes described here are fast compared to other effects in the cytoskeleton.

The model is valid under the assumption (11) on the parameters, which can be rewritten as the condition

$$\frac{1}{k_p} > \frac{1}{k_b \bar{\rho}} + \frac{1}{k_d},$$

on the relaxation time for polymerization on the one hand, and the sum of the relaxation times for binding of free gelsolin and for depolymerization on the other hand. Note however that for the binding reaction, $1/(k_b \bar{\rho})$ is the minimal relaxation time since $\bar{\rho}$ is the maximal density of free gelsolin molecules. For smaller densities of free gelsolin molecules, the relation can be reversed. This competition between polymerization and depolymerization is the essence of our model. Note that if a limit is approached, where the above inequality becomes an equality, the maximal filament length x_∞ (and therefore also the mean filament length $x_\infty/3$) tends to infinity by the dominance of the polymerization effect.

References

- [BLN79] Cl. Bardos, A.Y. Leroux, and J.C Nedelec. *First order quasi linear equations with boundary conditions. Comm. PDE*, 4:1017–1034, 1979.
- [Fla08] Ch. Flamm. *Models for the length distribution of actin filaments*. Master’s thesis, University of Vienna, 2008.
- [JG91] K.T. Joseph and G.D. Veerappa Gowda. *Explicit formula for the solution of convex conservation laws with boundary data. Duke Math. J.*, 62(2):401–416, 1991.
- [Lax57] P. D. Lax. *Hyperbolic Systems of Conservation Laws II. Comm. Pure and Applied Math.*, 10:537–566, 1957.
- [LeF88] P. LeFloch. *Explicit formula for scalar non-linear Conservation Laws with boundary condition. Meth. Applied Sciences*, 10:265–287, 1988.
- [LeV04] R.J. LeVeque. *Finite Volume Methods for Hyperbolic Problems*. Cambridge University Press, 2004.
- [Liu77] Tai-Ping Liu. *Large time behavior of solutions of Initial and Initial-Boundary value problems of a general system of Hyperbolic Conservation Laws. Comm. Math. Physics*, 55:163–177, 1977.
- [ÖS09] D. Ölz and Ch. Schmeiser. Cell mechanics: from single scale-based models to multi scale modeling, chapter *How do cells move? Mathematical modeling of cytoskeleton, dynamics, and cell migration*. Chapman and Hall/ CRC press 2009, 2009.
- [RBM⁺08] J. Roland, J. Berro, A. Michelot, L. Blanchoin, and J.-L. Martiel. *Stochastic Severing of Actin Filaments by Actin Depolymerizing Factor/Cofilin Controls the Emergence of a Steady Dynamical Regime. Biophys. J.*, 94:2082–2094, 2008.
- [SSVR02] J.V. Small, T. Stradal, E. Vignall, and K. Rottner. *The lamellipodium: where motility begins. Trends Cell Biology*, pages 112–120, 2002.
- [SXPM99] D. Sept, J. Xu, T.D. Pollard, and J.A McCammon. *Annealing accounts for the length of actin filaments formed by spontaneous polymerization. Biophysical J.*, 77:1911–1919, 1999.

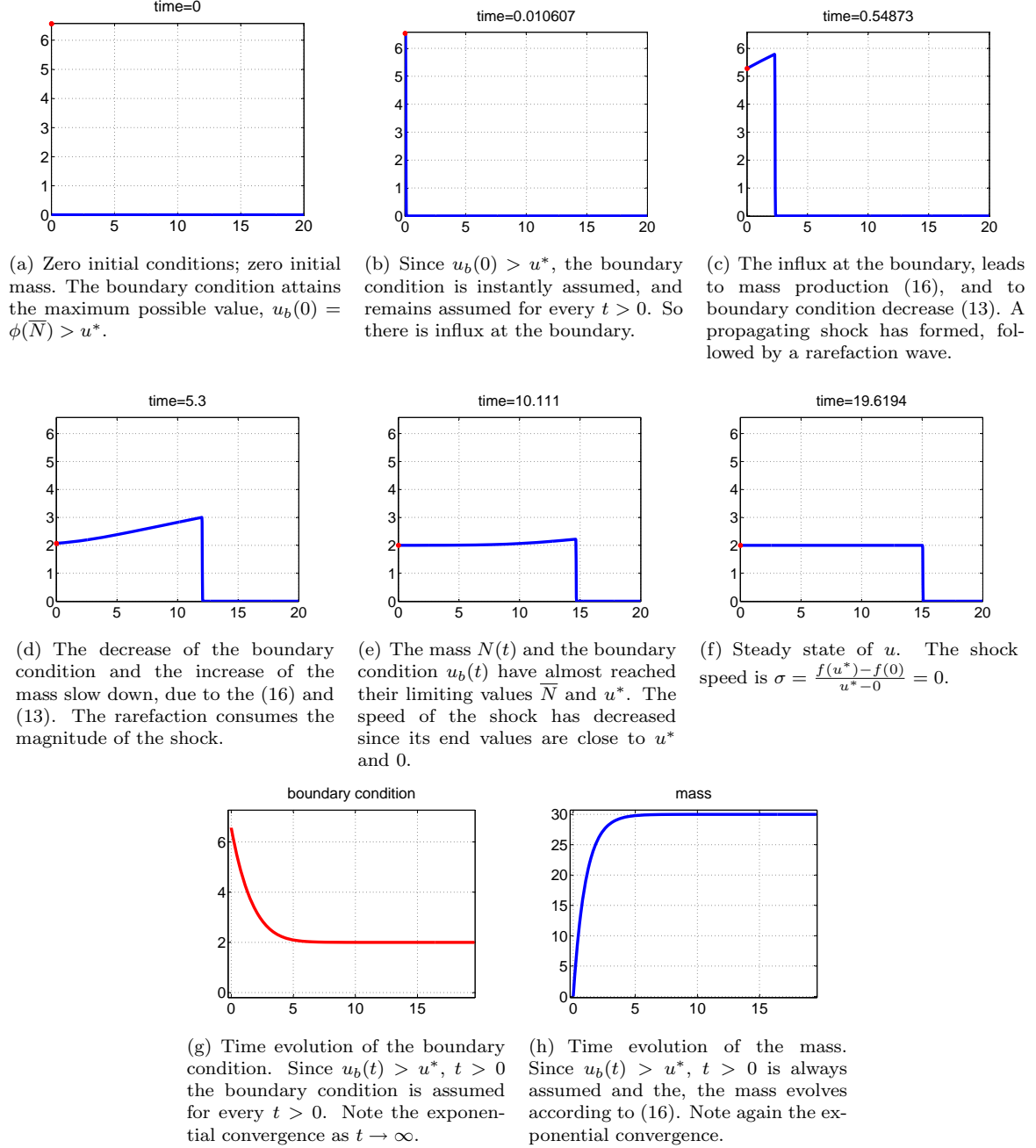


Figure 3: Numerical test 1. In this case $\bar{N} = 30$, the flux function $f(u) = u(u - 2)$, with $u^* = 2$ and the initial conditions are zero. As the Theorem 2 predicted, the boundary condition and the mass converge as $u_b(t) \rightarrow u^*$ and $N(t) \rightarrow \bar{N}$ respectively, and the asymptotic profile of u is a single steady shock at $x_\infty = \frac{\bar{N}}{u^*}$ with jump from u^* to 0.

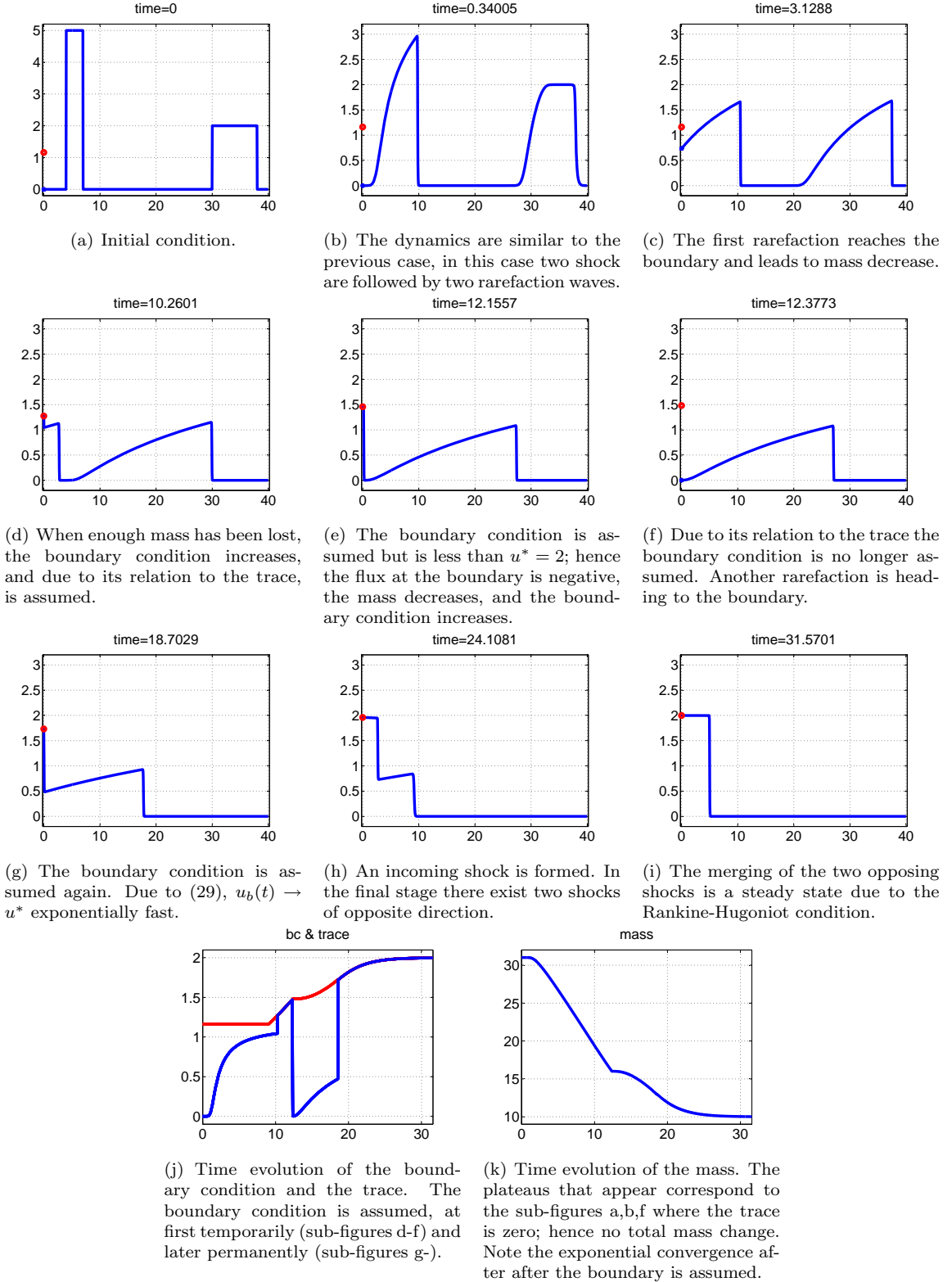
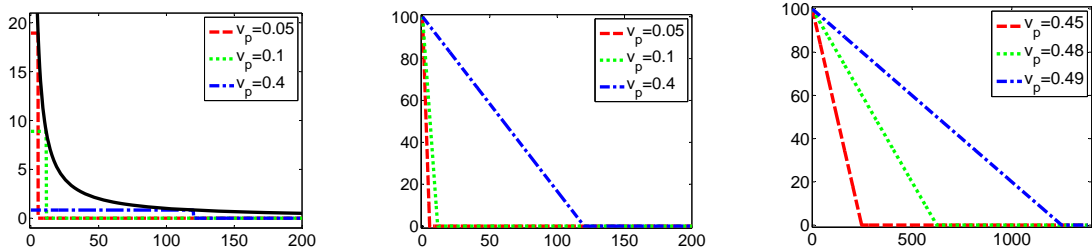


Figure 4: Numerical test 2. In this case $\bar{N} = 10$, and $f(u) = e^u - \frac{\epsilon^2-1}{2}u - 1$ with $u^* = 2$. The initial mass is larger than \bar{N} ; in this case the generalized model and the Theorem 6 predict the evolution.

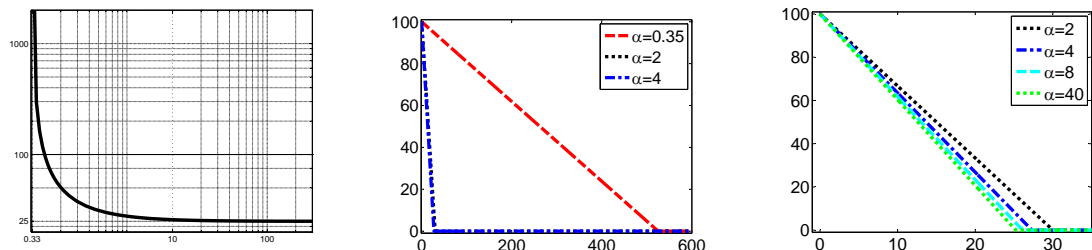


(a) We present the steady state density profiles u_∞ for $\alpha = 1$ and for various values of v_p (dashed lines), as a function of x . We also present the curve (x_∞, u^*) (solid curve) as a function of v_p , with $\alpha = 1$. We note that the discontinuities of the steady state shock wave solutions, coincide with the the (x_∞, u^*) curve.

(b) The steady state length distribution of the filament ends as functions of x . The total number of filaments is the same in all cases, coinciding with $\bar{N} = 100$, and the length of the filaments is distributed uniformly between $x = 0$ and $x = x_\infty$.

(c) The maximum length of filaments x_∞ tends to ∞ as v_p tends to its upper bound, which is $\frac{\alpha}{\alpha+1} = \frac{1}{2}$ in this case.

Figure 5: Numerical test 3. We study in this test, the steady state of the density and of the length distribution of the filament end points, as functions of v_p . We consider $\alpha = 1$ and $v_p = 0.05, 0.1, 0.4, 0.45, 0.48, 0.49$. We conclude that the higher the polymerization/depolymerization ratio v_p is, the larger the maximum filament lengths x_∞ are, more specifically we verify numerically that $\lim_{v_p \rightarrow \frac{\alpha}{\alpha+1}} x_\infty = \infty$.



(a) We present the graph of x_∞ as a function of $\alpha > \frac{1}{3}$ in logarithmic scales. We note the convergence of x_∞ at the endpoints its domain.

(b) We present the length distribution of the filament ends, for $\alpha = 0.35, 2, 4$, as functions of x . We note the large value of x_∞ for $\alpha = 0.35$. The total number of filaments is $\bar{N} = 100$. The length of the filaments is distributed uniformly between $x = 0$ and $x = x_\infty$.

(c) The same graph for other values of α . We note the convergence of x_∞ as α increases.

Figure 6: Numerical test 4. We study in this test, the steady state of the length distribution of the filament end points, for fixed $v_p = \frac{1}{4}$ and variable α . We conclude that the smaller the α , the longer the filaments are, i.e $\lim_{\alpha \rightarrow \frac{1}{3}} x_\infty = \infty$, on the contrary, the maximum filament length is bounded for large values of α , i.e $\lim_{\alpha \rightarrow \infty} x_\infty = 25 = \bar{N} v_p$.